05AC-120

Assessment of Eutectic Solder Phase Growth in Under-The-Hood Power Control Modules

Craig Hillman
DfR Solutions

Andre Kleyner
Delphi Delco

ABSTRACT

In many applications, especially automotive, solder interconnects experience degradation due to prolonged temperature and power cycling. This degradation behavior manifests itself as changes in the grain/phase structure, primarily through grain/phase coarsening. Because the magnitude of the change in grain/phase structure is strongly dependent upon the environmental stresses, quantifying microstructural changes provides an alternative approach to calculating an acceleration transform number or function. To verify this theory, Pb-rich regions in units subjected to accelerated life testing were compared to Pb-rich regions in units retrieved from the field with the intent of providing a linear correlation between their corresponding phase coarsening behavior.

INTRODUCTION

There are two fundamental forces that drive grains/phases in polycrystalline materials to grow. Grains coarsen because grain boundaries are areas of high potential energy. During grain coarsening, as grains grow larger, the total grain boundary area decreases, which, in turn lowers the free energy of the system. Particles with smaller size tend to combine into a larger particle with a lower total interfacial energy. Grain growth is driven by the local boundary curvature and the presence of triple junctions, which remain in equilibrium and act as anchors to grain boundary mobility [1].

In multiphase systems, such as eutectic solder, the thermodynamic basis of phase coarsening is a combination of the driving force for grain coarsening and the Thomson-Freundlich solubility relationship [2]. According to this relationship, the solute concentration in the matrix adjacent to a particle will increase as the radius of curvature of the interface decreases. Thus, the solubility in the matrix in contact with a β particle increases as the radius of the β particle decreases. This results in the formation of concentration gradients in the matrix, which cause the solute to diffuse in the direction

of the largest particles and away from the smallest particles. As the flow of solute proceeds, the small particles dissolve to compensate for the decrease in concentration at their interface. Likewise, the solute migrating towards the larger particles will precipitate at the particles and remove the excess solute arriving as the diffusion flux. Consequently, phase coarsening causes small particles to shrink and large particles to grow. This competitive growth and dislocation process will continue in theory until the system is completely phase separated.

The limiting factor in grain/phase growth is the application of sufficient thermal or mechanical energy. High temperatures supply thermal energy and mechanical energy is supplied by the application of stress, both cyclic and static. The rate of grain coarsening increases with application of thermal energy, because increased diffusion allows for more rapid movement of grain boundaries. Coarsening due to the application of mechanical energy occurs when the stress levels result in plastic deformation. Plastic deformation results in the production of an excess concentration of vacancies, which creates additional paths for material transport across phase boundaries. In binary alloys, coarsening during temperature cycling below the eutectic may also occur because of changes in the miscibility of the two phases [3].

There are two driving forces for solder phase growth during thermo-mechanical cycling (TMC). First, due to its low melting point, the imposed strains during TMC will most likely exceed the elastic limit of the solder and produce plastic deformation. As discussed previously, the presence of plastic deformation leads to the formation of vacancies, which allow for an increased rate of diffusion. In addition, the relatively high solid solubilities of Pb in Sn and vice versa, especially at elevated temperatures, lead to microstructural instability due to coarsening mechanisms. These regions of inhomogeneous microstructural coarsening are known to be crack initiation sites. It is well documented that these types of microstructures in Sn/Pb alloys fail by the formation of a coarsened band in which a fatigue crack grows. By studying the microstructural coarsening, which occurs during cyclic loading, constitutive equations for accurately predicting the fatigue life of solder joints can be developed.

EXPERIMENTAL PROCEDURE

To correlate the effect of accelerated power temperature cycling (PTC) with field environment, the degradation of eutectic solder joints phase structure in both field and test environments was characterized. An estimation of the acceleration factor was attempted based on a comparison of solder degradation in PTC-exposed units with fielded units of known mileage and model year.

PART SELECTION

Twenty three automotive power-control modules (PCMs) retrieved from the field. Based on the type of components and their location on the circuit card, the twenty three modules were subdivided into six groups. Module information is displayed in Table 1.

Table 1: Listing of power modules

Group	Model Year	Mileage
New	2001	0
1	1996	53,640
	1997	62,800
	1996	78,650
2	1995	82,650
	1995	109,450
	1995	58,350
	1994	90,700
3	2000	23,800
	1999	38,400
	2000	14,200
	1999	32,000
4	1997	94,700
5	1998	48,500
	1998	36,200
6	1993	183,200
	1992	156,900
	1990	125,440
	1991	N/A
	1988	67,200
	1990	73,300
	1993	55,700
	1989	N/A
	1991	44,000

To ensure that proper and relevant comparisons could be made, parts were selected based on two criteria. The first was that the part had to be assembled on a majority of the modules. The second criterion was that the part had the potential to be susceptible to failure due to solder joint fatigue. The parts selected included axial-leaded diodes, L-leaded tantalum capacitors, chip resistors, J-leaded plastic microcircuits, and gull wing-leaded components. Part information is given in Table 2.

Table 2: List of parts selected for solder grain size measurements

Part Type	Lead	Package	Case Size (mm)	Image
PEM	J-lead	N/A	11 x 11 x 4	
PEM	Gullwing	MS-022AB	9.5 x 9.5 x 2.5	
PEM	Gullwing	N/A	27.2 x 17 x 2	
Diode	Axial	N/A	17 x 4 x 4	
		N/A	22 x 4 x 4	
Resistor, Thick-Film	Leadless	2010	5 x 2.6 x 0.6	
Diode, Glass	Leadless	SOD80C	3.7 x 1.6 x 1.6	
		N/A	5.5 x 3.3 x 3.0	
Capacitor, Tantalum	L-lead	Case B	3.3 x 3.0 x 1.7	
		Case D		

ACCELERATED THERMAL CYCLING

In addition to the twenty-three field units, thirty newly constructed PCMs, model year 2001, were provided for accelerated life testing. The PCMs were subjected to the temperature profile detailed in Figure 1. One cycle consisted of approximately 60-minute dwells at -40ºC and at 135ºC and ramp rates of approximately 10ºC per minute, for a total cycle time of approximately 2.5 hours. Two PCMs were removed from the test chamber every 200 hours for analysis.

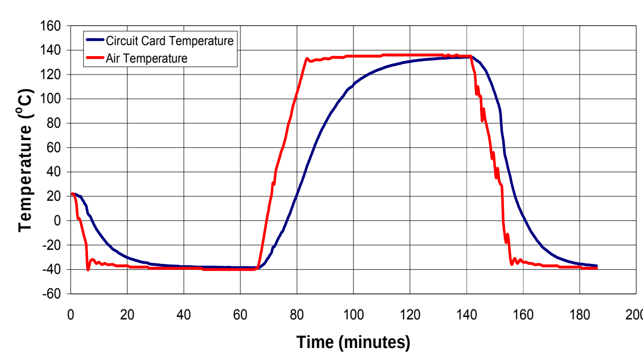

Figure 1: Temperature profile for accelerated life testing of power control modules

SAMPE PREPARATION

For phase size measurement on all 23 field PCMs and approximately 20 test PCMs, three to seven components were selected per PCM. As a baseline, one new module was also selected for cross sectioning. The area of the module with the component of interest was sectioned out and potted in a room temperature cure epoxy resin. This insured that there was no relative motion of the part with respect to the board.

After the potting mixture solidified, coarse silicon carbide (SiC) grinding paper, 240 and 400 grit, was used to reach the area of interest. Fine grinding paper, 600 and 800 grit, was used to prepare the cross-section for polishing. During grinding, the water was the lubrication medium of choice and the time required was approximately 1 to 2 minutes. The final step in grinding was very fine 1200 grit to remove any damage remaining from the coarser grit.

Initial polishing consisted of 1.0 or 0.3 micron size alumina powder suspended in distilled water. This step required approximately 60-120 seconds and was completed when no surface damage, such as scratches, were visible. The final step involved either 0.05 micron alumina or colloidal silica. Both polishing media attack the lead-rich and tin-rich regions at different rates, greatly increasing the micro structural contrast.

PHASE MEASUREMENT

Optical images of the solder joints of interest were obtained using a Zeiss Axiovert 135 with a Diagnostic Instruments Spot Digital Camera with 1.1-megapixel resolution. For phase size measurement, all solder joints were imaged at 200x. Magnification of 200x was selected, because it was the highest magnification that still captured the entire solder joint. The pixel density of the 4" x 5" optical images was 263 pixels/inch. At 200x, this limits the pixel area to approximately 5 μm^2.

Phase area was measured using the UTHSCA Image Tool 3.0. Phase size measurements were taken from one solder joint for each component, because the adjacent solder joints often showed similar phase structure and size. Phase diameter was taken as a square root of the area, which assumed that the average grain was approximately square in shape. Because phase size measurement requires discontinuous areas, the dark or lead-rich phases were used for phase size measurement.

Before the pictures could be analyzed it was necessary to crop the solder joint region. This was because the coloration of the adjacent areas was often similar to the dark lead-rich phases, leading to errors in phase area identification. In addition, because the UTHSCA Image Tool is only capable of differentiating between black and white regions, color was removed from the image. An example of the process is shown in Figure 2.

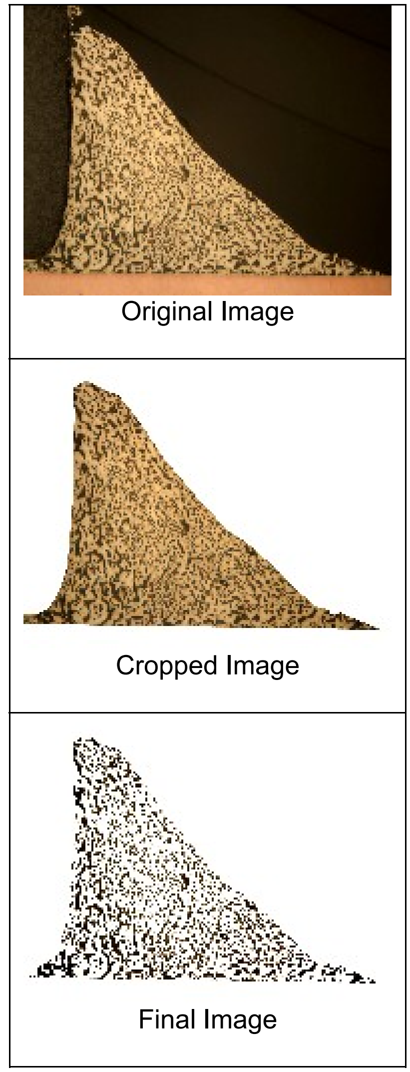

Figure 2: Image preparation for phase size measurement

RESULTS

The results of this study are provided in two forms. The first form is a comparison of the morphology of the solder joints subjected to field and test conditions. The second result is an analysis of the Pb-rich phase size in attempt to predict phase growth behavior and develop an acceleration factor.

Because of the large number of solder joints, approximately 300, that were documented during this project, comparison of solder joint morphology was primarily focused on those parts that experienced void coalescence and crack propagation during accelerated

life testing. This consisted of the axial-leaded diode and the 2010 chip resistor.

SOLDER JOINT MORPHOLOGY

Solder joint void coalescence and crack propagation were first observed on an axial-leaded diode after 600 temperature cycles (see Figure 3). While the axial-leaded diode was the first to show damage accumulation, the extent of crack propagation remained relatively constant with increasing temperature cycles. This is due to the architecture of an axial-leaded through-hole solder joint, which results in stress relaxation after the initial radial crack propagation.

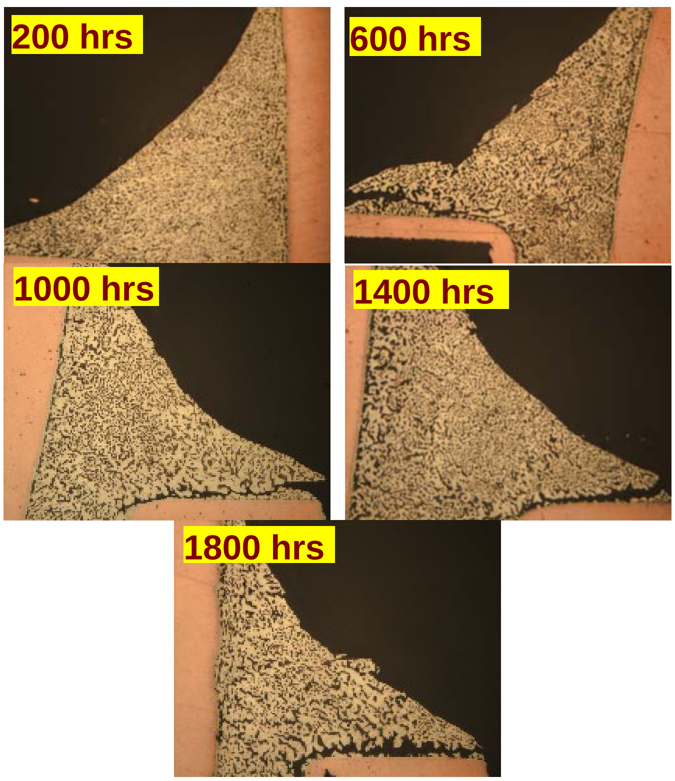

Figure 3 (60x): Optical micrographs of cross-sectioned axial-leaded diode solder joints subjected to temperature cycling (Figure 1).

A comparison the solder joint morphology seen on the field units subjected to the most extreme conditions (oldest model year or highest mileage), as displayed in Figure 4, clearly shows that the test units after 600 hours of exposure have experienced a higher degree of Pb-rich phase coarsening. This is especially observable along the axial lead and board bond pad interfaces.

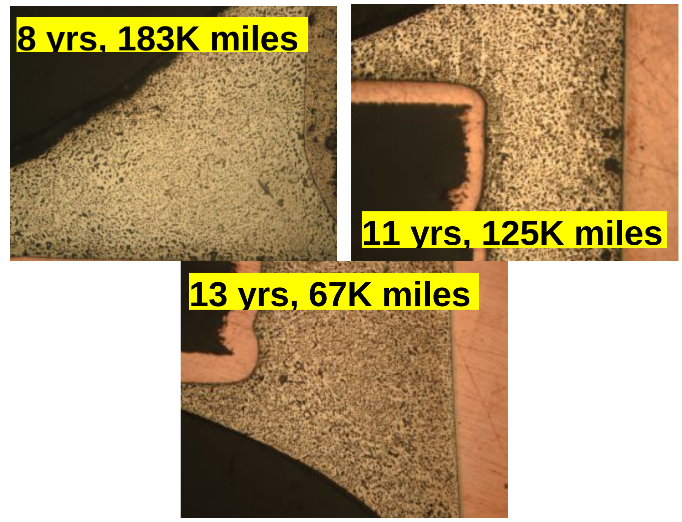

Figure 4 (60x): Optical micrographs of cross-sectioned axial-leaded diode solder joints from power control modules retrieved from the field

The first solder joint identified as having crack propagation extensive enough to result in electrical failure was a 2010 chip resistor after 1800 hours of temperature cycling, shown in Figure 5. Unlike the axial-leaded diode, the phase coarsening seen in the test unit is similar in dimension to the phase coarsening seen in the units fielded for 11 and 13 years (see Figure 6). However, in the test units, the phase coarsening is location specific, primarily along the regions of highest shear stress. In the field units, the location of the phase coarsening is randomly distributed throughout the solder joint. Considering the shape of the solder joint, bulbous with a concave surface profile, and the time in the field, the phase coarsening observed in the field units were most likely the result of slow cooling after reflow and long-term exposure to elevated temperatures rather than experiencing thermomechanical stresses during operation.

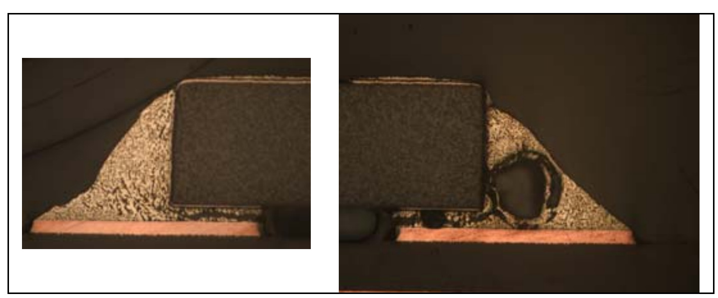

Figure 5: Optical micrographs of cross-sectioned 2010 chip resistor solder joints after exposure to 1800 hours of temperature cycling (see Figure 1).

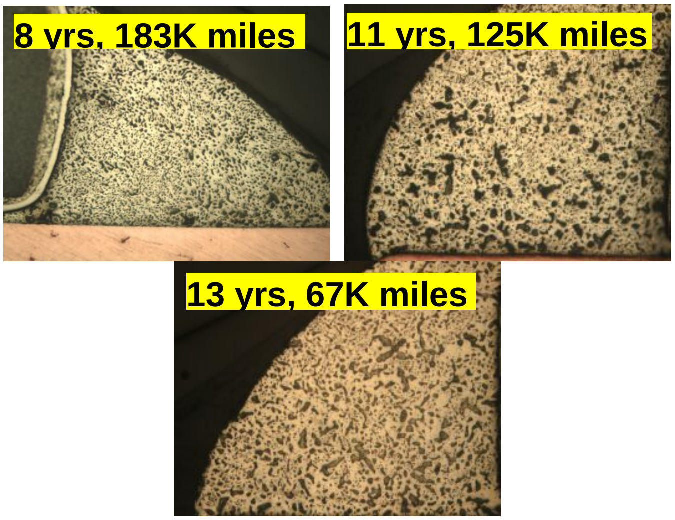

Figure 6 (80x): Optical micrographs of cross-sectioned 2010 chip resistor solder joints from power control modules retrieved from the field

The results of comparing Pb-rich phase evolution in the test units to the field units seems to show that the amount of damage being applied after approximately 600 hours of -40 to 135oC temperature cycling exceeds the damage experienced after 183,000 miles or 13 years in the field. These initial findings must be tempered with the realization that the 23 PCMs examined represent a small fraction of actual production and there may be environments or driving habits where the PCMs experience a higher level of thermomechanical stress.

An attempt to develop an acceleration factor from phase coarsening behavior can now be benchmarked against the onset of crack initiation at 600 hours. That is, the acceleration factor would have to predict that 600 hours of test time applies a greater degree of damage then 183,000 miles or 13 years in the field.

PB-RICH PHASE GROWTH BEHAVIOR

For each part, the mean phase diameter was found using descriptive statistics (σ, ρ and μ). The best fit was found to be a log-normal distribution

$$Q(t) = \frac{1}{\sigma\sqrt{2\pi}} \int_0^t \left(\frac{1}{x} \exp\left[\left(\frac{-1}{2} \right) \left(\frac{\ln x - \mu}{\sigma} \right)^2 \right] dt \right)$$

For each power control module, an average phase diameter was calculated from each parts' mean phase diameter. The average phase diameter for both field and test units was plotted as a function of time of exposure. The results are displayed in **Error! Reference source not found.** and **Error! Reference source not found.**.

The change in phase diameter as a function of time of exposure was found to display a power law behavior, with a relationship of

$$d = Ct^{0.12}$$

for both the field and test units, where C is an empirical constant. Using the constants derived from the data in **Error! Reference source not found.** and **Error! Reference source not found.** results in a calculated acceleration factor of approximately 50,

$$\left(\frac{8}{5} \right)^{1/0.12} = 50$$

Using the evolution of the Pb-rich phase diameter as a basis, this would imply that a test time of 2,000 hours is roughly equivalent to 100,000 hours in the field (~12 years). As straightforward as this exercise would seem, this result is not valid as it conflicts with the observation of void coalescence and crack initiation in the test units, described in previous section. Based on the comparison of field and test unit solder joint morphology, a minimum acceleration factor of approximately 200 is expected[1].

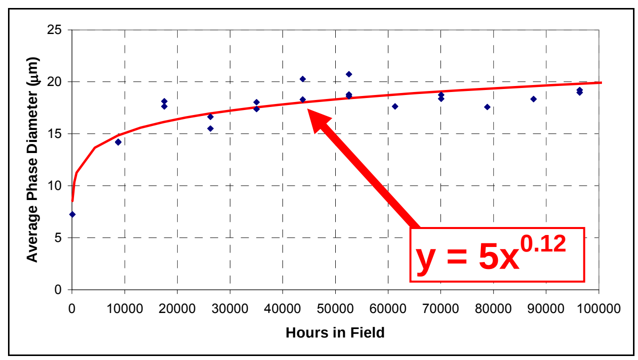

Figure 7: Average diameter of the Pb-rich phase in solder joints from field PCMs

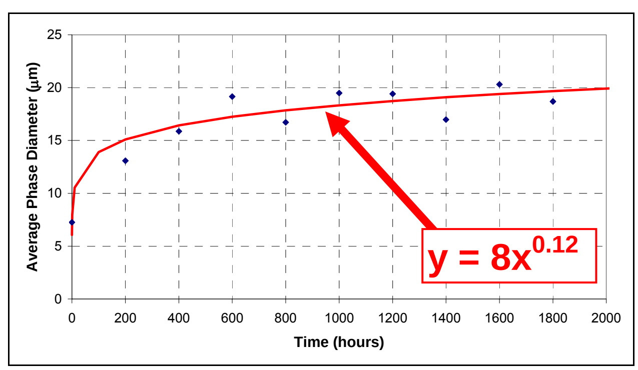

Figure 8: Average diameter of the Pb-rich phase in solder joints from PCMs subjected to thermal cycling (see Figure 1)

[1] 600 hours under test being equal to or greater than 13 years (114,000 hours) in the field,

DATA SEGREGATION AND ASSESSMENT

Because of the large amount of data being acquired, 300 solder joints with 750 to 2500 distinct phases per solder joint, the attempt to track phase coarsening through averaging may have resulted in more appropriate information being masked. When solder joints are subjected to thermomechanical stresses, especially temperature cycling, phase coarsening is a localized phenomenon, primarily occurring in the region with the highest shear stresses. Limiting phase diameter comparison to these critical phases may provide more insight on the correlation between field environments and test conditions.

Following this philosophy, the thirty largest phase diameters in each solder joint were plotted as a function of model year and a parameter labeled as miles-hours (see Figure 9 and Figure 10, respectively). Use of the independent variable miles-hours was an attempt to include the dual effects of temperature rise due to engine operation (mileage) and temperature rise due to diurnal cycles (years in the field).

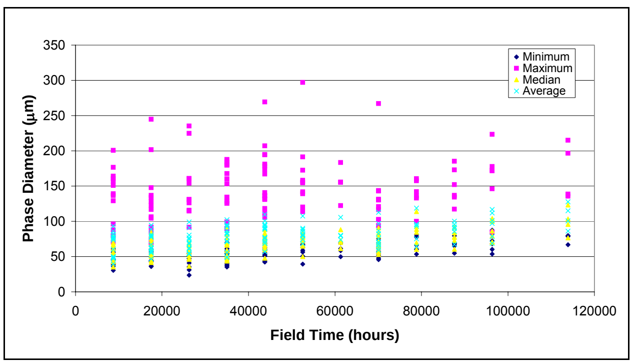

Figure 9: Plot of the minimum, maximum, median and average of the thirty largest phase diameters as a function of model year (field time)

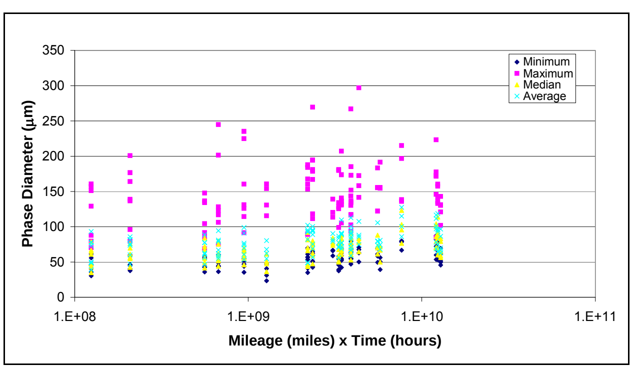

Figure 10: Plot of the minimum, maximum, median and average of the thirty largest phase diameters as a function of miles-hours.

The results seemed to show that the change in the average phase diameter, for the thirty largest phases, shows a consistent increase as a function of miles-hours. This modified average phase diameter was then used as a correlation to the test units. Based on observations of the solder morphology, it would be expected that the average of the thirty largest phases at 400-600 hours, shown in Figure 9, should be roughly equivalent to 1 x 10^{10} miles-hours. The actual correlation was found to be far smaller. Observing the data in Figure 11 and Figure 12, the average of the thirty largest phase diameters in the test units at 2000 hours under test comparable to the average phase diameter at 2 x 10^{8} miles-hours (10,000 hours and 20,000 miles).

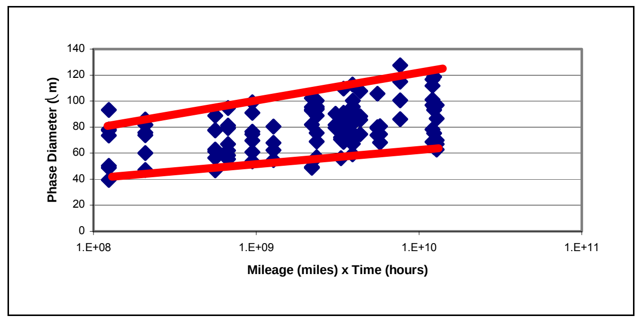

Figure 1: Plot of the average of the thirty largest phase diameters as a function of miles-hours.

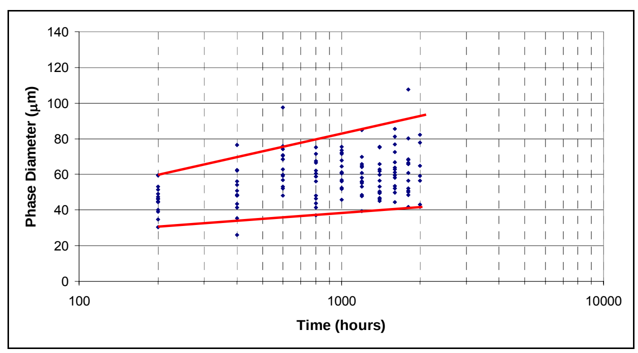

Figure 2: Plot of the average of the thirty largest phase diameters as a function of time under accelerated life testing (see **Error! Reference source not found.**).

A final approach was to normalize the independent parameters, time in the field or mileage, based on usage models. Examples of these usage models are displayed in Table 4. However, since all of these models assume a linear dependence upon either time in the field or mileage, data normalization was found to have a minimal effect.

Table 4: Models describing usage of American automobiles

Model	Normalization Factor	Comments
Number of usage hours per year in the field	385 hours[2]	Median behavior
Number of usage hours per mile	0.051 hours[3]	Assumes an average speed of 19.6 mph
	0.029 hours[4]	Assumes an average speed of 34 mph
Number of use cycles per year	1825 cycles	Assumes 5 trips per day

DISCUSSION AND CONCLUSION

The current techniques used to quantify coarsening of phase diameter do not seem to be an effective assessment of life remaining and were not capable of providing a defensible acceleration factor. There seem to be three potential drivers for this conclusion:

First, the nature of phase growth will make the acceleration factor variable depending on where in the process the measurement is made. As seen in Figure 13, the rate of phase growth will differ in the test and field units. This variable behavior will result in different ratios depending upon where in the coarsening stage the measurement is performed. Since the only acceleration factor of actual concern is the ratio of the time to failure, acceleration factors based on phase coarsening could result in a reduced value, as observed during this analysis.

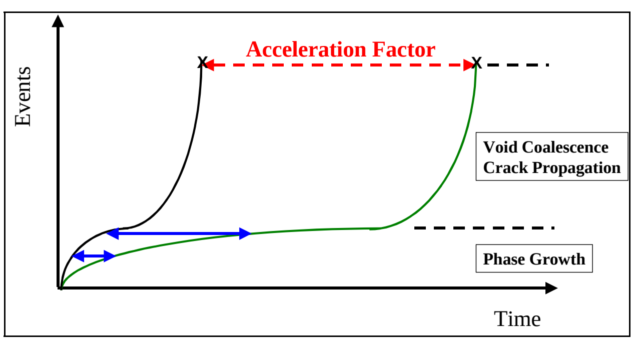

Figure 13: Schematic of variability in phase growth rates

Second, phase growth is not necessarily a precursor to crack initiation. If an excessive amount of solder is applied during manufacturing, the solidification rate will be slower than a nominal solder joint. This will result in greater phase separation and a corresponding increase in Pb-rich phase diameter. This was seen in Figure 6. In addition, long-term exposure to elevated temperatures, e.g. parked outside in Phoenix, could also result in extensive phase coarsening without damage accumulation (see Figure 14).

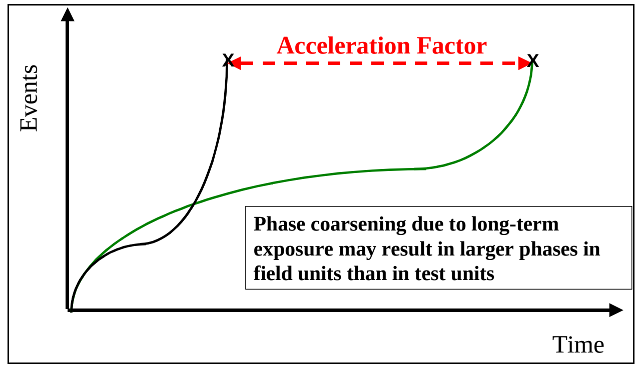

Figure 14: Schematic of long-term exposure at elevated temperatures on differentiation in phase/grain size

Finally, phase growth and crack initiation does not necessarily indicate near-term failure. The geometry of the solder joint and the thermo-mechanical stress being applied could result in crack propagation that results in stress relaxation, rather than an acceleration of the degradation process. This was observed with the axial-lead diodes displayed in Figure 3. While the stress state induces cracking along the solder/board bond pad interface, this cracking induces a sufficient relaxation of internal stresses that additional crack propagation is greatly retarded before circumferential cracking down the filled barrel can initiate.

Based upon examination of solder joints from field and test power control modules and analysis of phase coarsening behavior, 3000 hours of accelerated temperature cycling (-40 to 135ºC) would seem to be excessive in relation to crack initiation (axial leaded diode) and first solder joint failure (chip resistor). A time frame of 600 hours would seem to be more appropriate for the given field environment.

ACKNOWLEDGEMENTS

The research for this paper was performed at the University of Maryland. The authors would like to thank Delphi Delco for supplying the samples used for this investigation. A special thanks to M. Marino for his efforts in sample preparation and Abhijit Dasgupta for several helpful discussions.

REFERENCES

1. H.V. Atkinsen, "Theories of Normal Grain Growth in Pure Single Phase Systems," Acta Met., V. 36 (1988), pp.469-491.
2. K. Lucke, G. Abbruzzese, and I. Heckelmann, "Statistical Theory of 2-D Grain Growth Based on First Principles, and its Topological Foundation", Mat. Sci. Forum 94 (1992), pp. 1-16.
3. H. Abubauer, "Acceleration of Coarsening by Cycling of Temperatures," Scripta Metallurgica, vol. 12, pp. 1003-6, 1978.

[2] Source: DelphiDelco
[3] Source: U.S. Environmental Protection Agency
[4] Source: U.S. Department of Transportation

CONTACT

Dr. Craig Hillman is the President and CEO of DfR Solutions (www.dfrsolutions.com), a leading failure analysis and reliability consultancy. Dr. Hillman and his experienced staff, with a wide variety of expertise, provide rapid, turnkey solutions for the electronics industry. Dr. Hillman was formerly a research associate at the University of Maryland. During his tenure, Dr. Hillman developed an international reputation as an expert in issues with Pb-free, identifying root-cause of failures in electronics, capacitor behavior and failure modes, conductive anodic filament (CAF) formation, electrochemical migration/ dendritic growth, and general reliability issues. Dr. Hillman has used his fundamental understanding of product failure to develop formalized rules for the design and manufacturing process. This has allowed DfR Solutions to provide services with a high return on investment, in such broad applications as component specifications, lifetime predictions, and material and technology qualification. Dr. Hillman has a B.S. in Material Science from Carnegie Mellon and a PhD in Materials from University of California-Santa Barbara. He can be reached at chillman@dfrsolutions.com or by calling 301-474-0607.

APPENDIX 1: SOLDER JOINT MORPHOLOGY, CHIP RESISTORS, FIELD UNITS

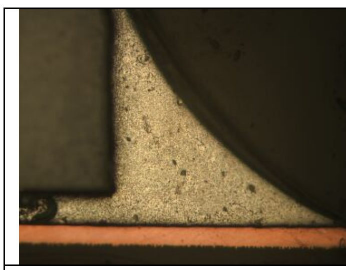
0 miles

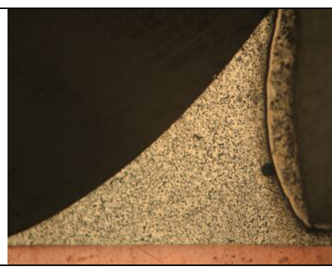
14200 miles, MY 2000

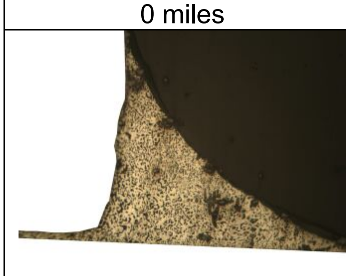
23800 miles, MY 2000

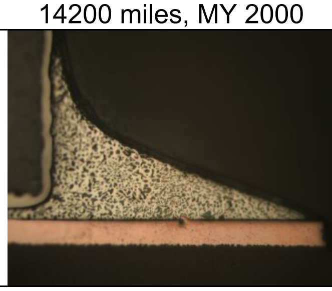
32000 miles, MY 1998

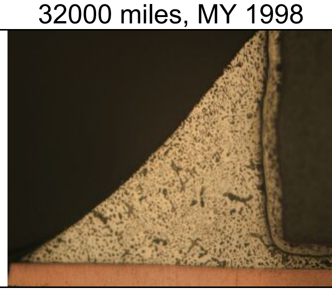
38400 miles, MY 1999

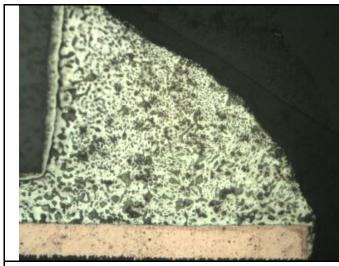
44690 miles, MY 1991


53640 miles, MY 1996

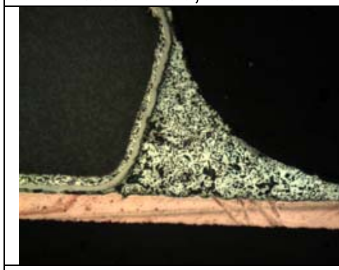
48500 miles, MY 1998


55700 miles, MY 1993

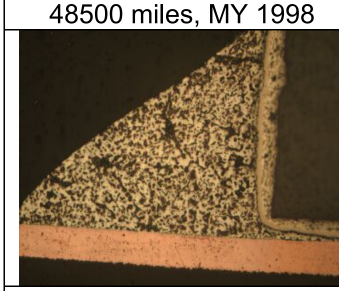
62800 miles, MY 1997


67200 miles, MY 1988

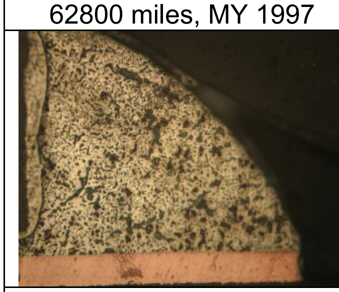
78650 miles, MY 1996


94700 miles, MY 1997

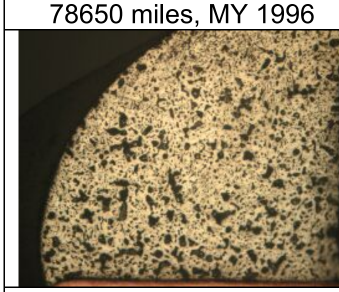
125440 miles, MY 1990


156900 miles, MY 1992

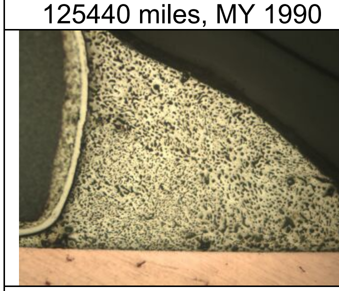
183200 miles, MY 1993

APPENDIX 2: SOLDER JOINT MORPHOLOGY, CHIP RESISTORS, TEST UNITS

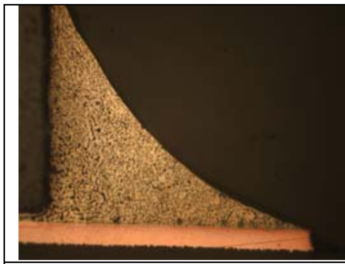

200 hours (Board M43338) | 200 hours (Board M43026)

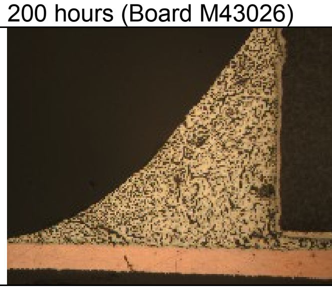

400 hours (Board M42174) | 400 hours (Board M43090)

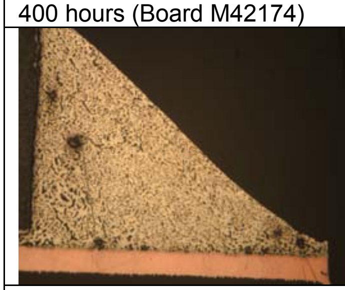

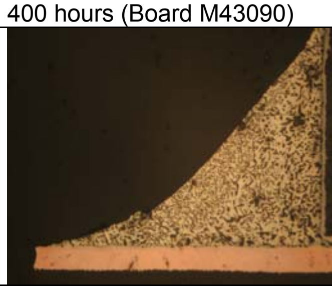

600 hours (Board M42829) | 600 hours (Board M43087)

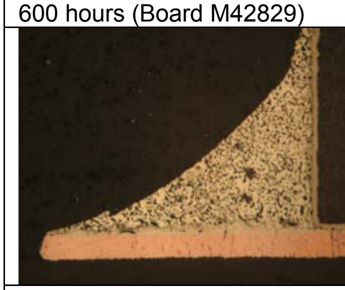

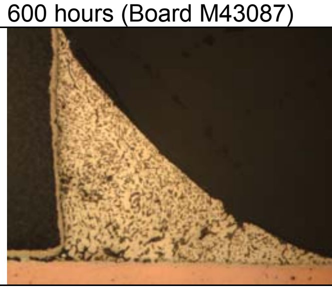

800 hours (Board M43331) | 800 hours (Board M41993)

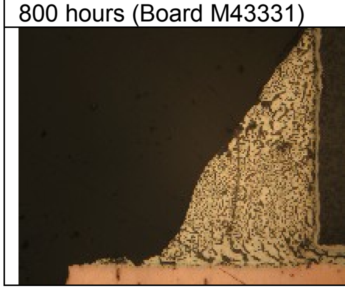

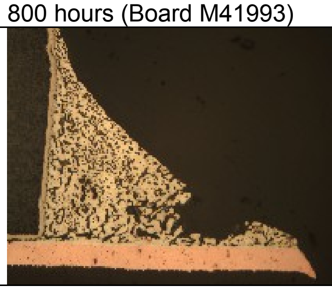

1000 hours (Board M42504) | 1000 hours (Board M41708)

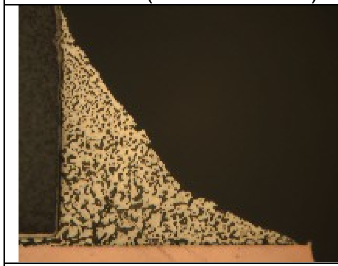

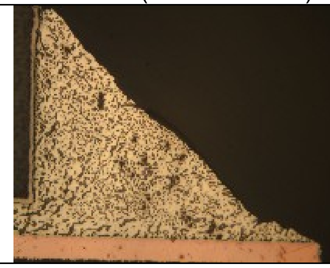

1200 hours (Board M42369) | 1200 hours (Board M41899)

1400 hours (Board M42736) | 1400 hours (Board M42548)

1600 hours (Board M41943) | 1600 hours (Board M42615)

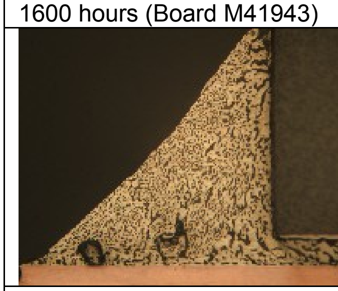

1800 hours (Board M42479) | 1800 hours (Board M27856)

2000 hours (Board M42459)